Supplementary Material. Topographically constrained interseismic uplift distribution

Here we compare observed and modeled river elevation profiles for 20 channels draining approximately perpendicular to the strike of the Himalayan Range Front (HRF) across PT_2 between 84°-87° east longitude and 27°-29° north latitude (Figure DR1). These channels were chosen to give a relatively evenly spaced distribution along the strike of the Nepalese segment of the HRF. A subset of the chosen profiles does not fully cross the topographic expression of PT_2 (e.g. channels 1, 2, 5, 9, 13, 19, 20). Elevations above 4 km are not considered due to the fact that glaciers may have recently modified them.

If interseismic deformation does indeed control the river profiles at the HRF then present day topography can be used to estimate the slip rate, locking depth, location, and fault dip of the interseismic uplift model in the same way that geodetic data have been traditionally used. Here we estimate the lateral and vertical position of the locked termination of the fault assuming that the fault slip rate and dip are fixed at 20 mm/yr and 4° respectively over the area of interest which is consistent with previously reported estimates based on geodetic data. While this estimator could be extended to solve for both slip rate (linear) and dip (non-linear) we have focused on the lateral and vertical position of the locked zone to explore how two non-linear parameters can be estimated. For each river elevation profile (derived from steepest descent analysis of 90-meter SRTM data) we use a systematic grid search to estimate the location of the locked zone (locking depth) assuming a fault slip rate of 20 mm/yr and a fault dip of 4°. The minimization criterion is a minimum length norm of 100 evenly spaced points along each elevation profile. For each of the 20 channels we solve for the best-fitting erosion coefficient, K, and the slope and drainage area/discharge exponents, n and m, respectively. We find average values of $\log_{10} K = -1.7 \pm 1.7$, $n = 1.4 \pm 0.2$, and $m = 0.5 \pm 0.2$. Note that we find a strong ($\rho = -0.98^{+0.01}_{-0.03}$) negative, linear, covariance between $\log_{10} K$ and m.

Channel elevations predicted by this interseismic uplift model exhibit the characteristic changes in slope and curvature observed in river profiles along the HRF (Figures DR2-21). While the model does not replicate all features at the <10 kilometer scale, the overall goodness of fit is quite good, with a mean residual of ~100 meters

elevation and a reduction in variance of 80% for the 20 major channels in our study area. The interseismic uplift model can successful predict the form of the river profiles that do not entirely cross PT_2 (channels 1, 2, 5, 9, 13, 19, 20, Figures DR1, DR2).

The spatial distribution of uplift along each river is estimated, independently of one another, and allows for the calculation of a topographically constrained uplift distribution (Figure DR23). The optimal value of the interseismic to block uplift is determined by a systematic grid search at different values of ϕ. The optimum value of $\phi = 0.8$ translates to only 20% of the accumulated interseismic deformation being released as earthquakes and a mean residual elevation of 72 meters (Figure 4 in main text). The goodness-of-fit decreases slightly with additional interseismic deformation but increases to 150 with even a modest increase in coseismic deformation to 50% of the interseismic level. This map is constructed by taking the predictions for uplift rate along each channel (as a function of longitude and latitude) and by using bi-cubic splines to interpolate inside the convex hull defined by the position of the planform location of channels 1-20. Rock uplift rates are only strictly estimated along each channel profile but this plot is useful to assess the lateral continuity of estimated uplift distribution. Due to the fact that the slip rate is assumed to be 20 mm/yr the peak uplift is approximately the same (8 mm/yr) for each profile. However, there appears to be a latitudinal kink in the uplift distribution at 86.75 degrees longitude. This is somewhat similar to, though approximately 30-50 km west of, the kink previously estimated using a denudation rate model (Lavé, J., and Avouac, J.P., 2001, Fluvial incision and tectonic uplift across the Himalaya of Central Nepal, *Journal of Geophysical Research*, 106, 26,561-26,591).

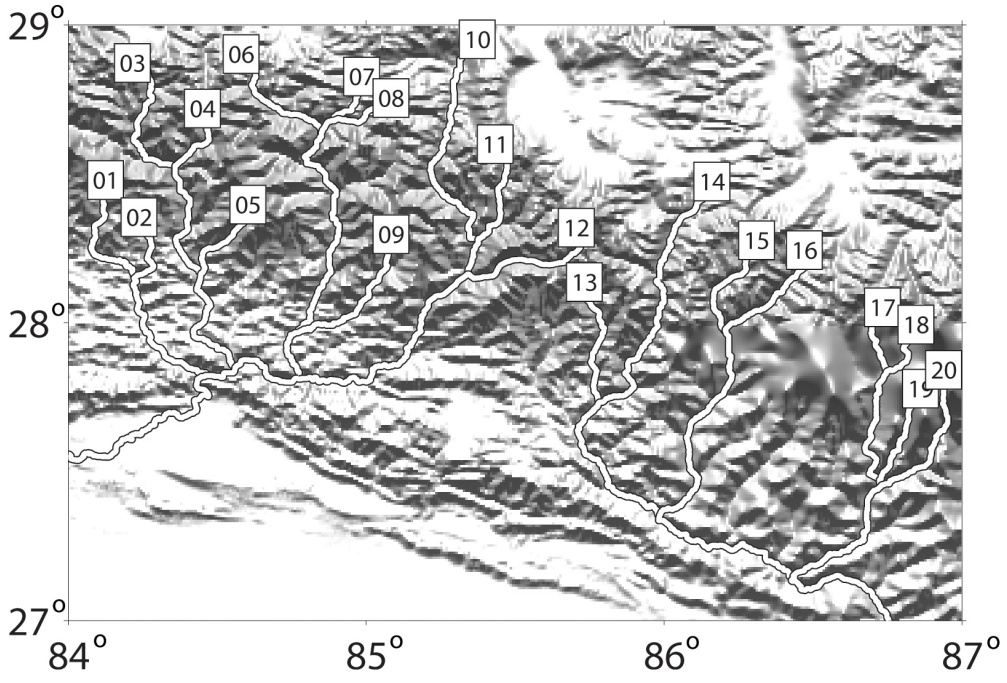

Figure DR1. Topography and channel locations along the Nepal segment of the Himalayan Range Front. Topography is shown as shaded relief and the channel paths are outlined in black. Each of the channels is labeled 1-20 with values increasing eastward.

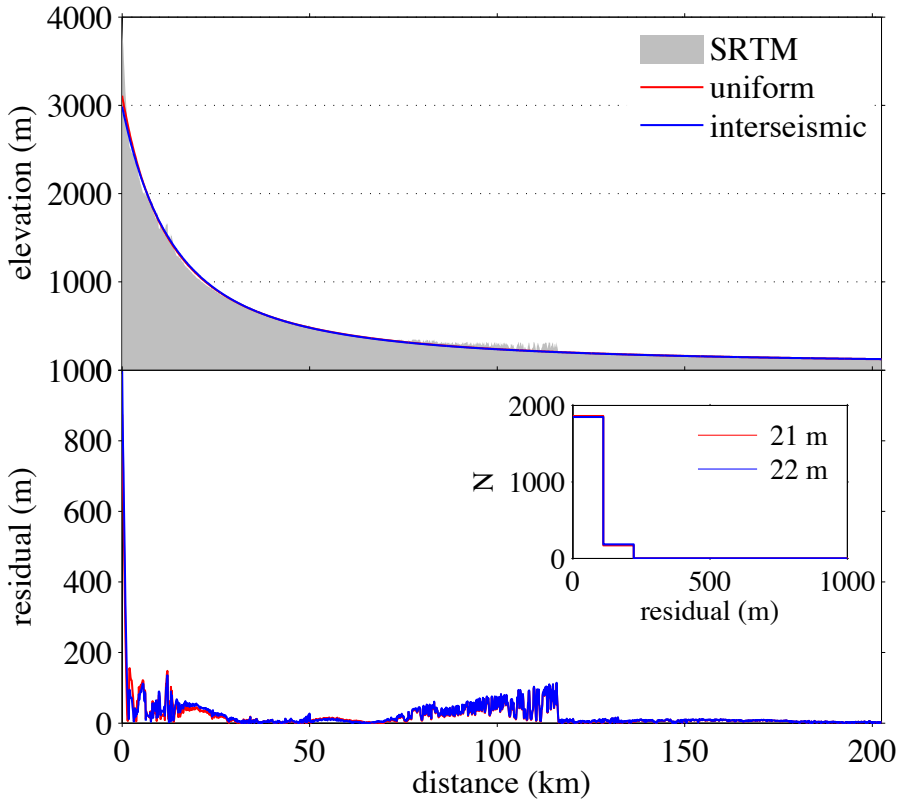

Figure DR2. Observed and modeled channel profiles for channel 1 in Figure DR1. Upper panel: Raw elevation data (SRTM) is shown in gray with uniform and excess interseismic rock uplift models in red and black respectively. Lower panel: magnitude of residual (SRTM-modeled) elevations for uniform (red) and excess interseismic (blue) rock uplift models. Residual elevation frequency distribution shown in inset. Legend gives the mean residual magnitude for uniform (red) and excess interseismic (blue) rock uplift models.

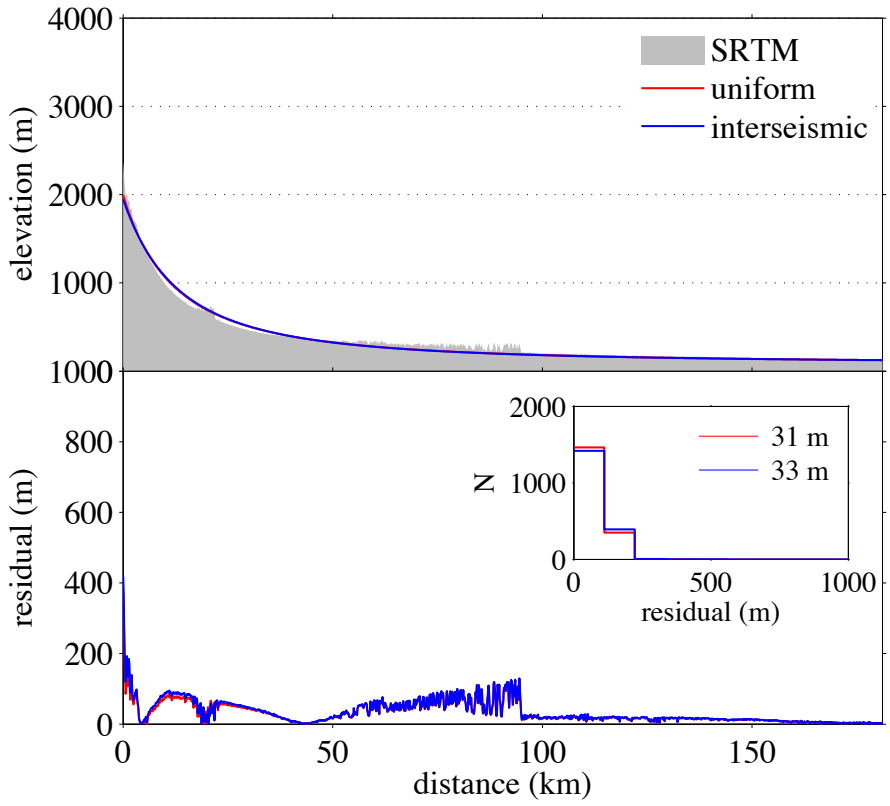

Figure DR3. Observed and modeled channel profiles for channel 2 in Figure DR1. Upper panel: Raw elevation data (SRTM) is shown in gray with uniform and excess interseismic rock uplift models in red and black respectively. Lower panel: magnitude of residual (SRTM-modeled) elevations for uniform (red) and excess interseismic (blue) rock uplift models. Residual elevation frequency distribution shown in inset. Legend gives the mean residual magnitude for uniform (red) and excess interseismic (blue) rock uplift models.

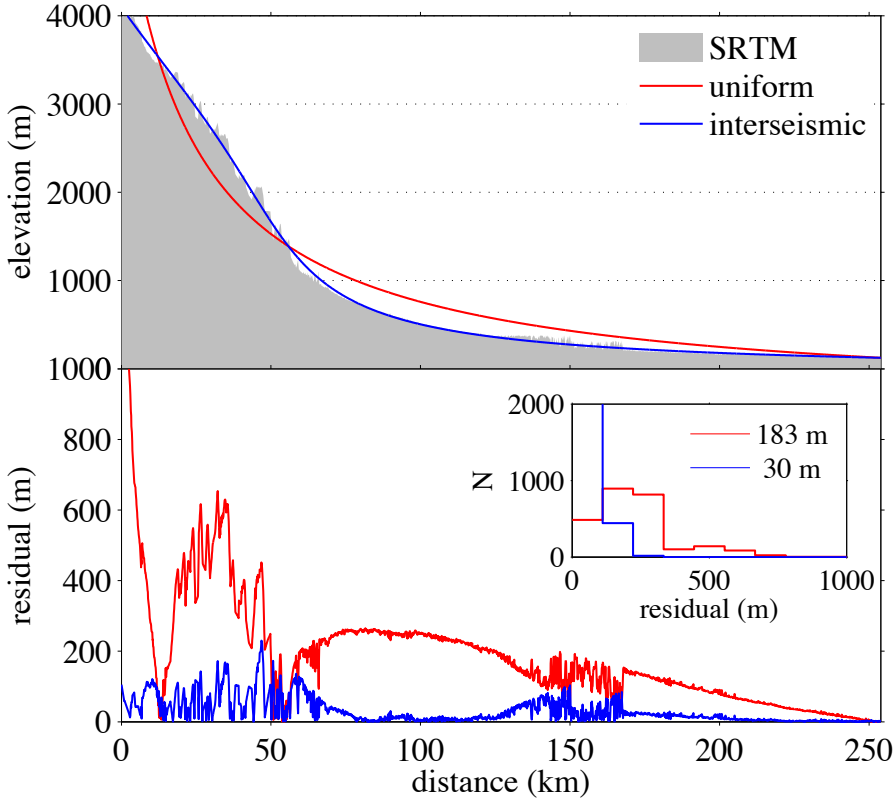

Figure DR4. Observed and modeled channel profiles for channel 3 in Figure DR1. Upper panel: Raw elevation data (SRTM) is shown in gray with uniform and excess interseismic rock uplift models in red and black respectively. Lower panel: magnitude of residual (SRTM-modeled) elevations for uniform (red) and excess interseismic (blue) rock uplift models. Residual elevation frequency distribution shown in inset. Legend gives the mean residual magnitude for uniform (red) and excess interseismic (blue) rock uplift models.

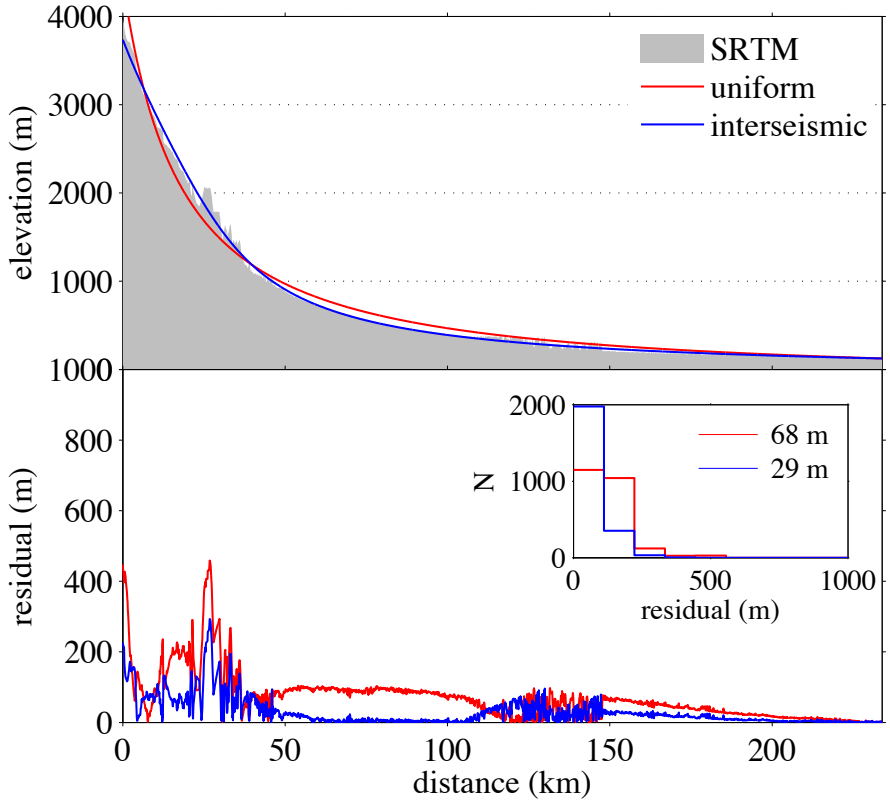

Figure DR5. Observed and modeled channel profiles for channel 4 in Figure DR1. Upper panel: Raw elevation data (SRTM) is shown in gray with uniform and excess interseismic rock uplift models in red and black respectively. Lower panel: magnitude of residual (SRTM-modeled) elevations for uniform (red) and excess interseismic (blue) rock uplift models. Residual elevation frequency distribution shown in inset. Legend gives the mean residual magnitude for uniform (red) and excess interseismic (blue) rock uplift models.

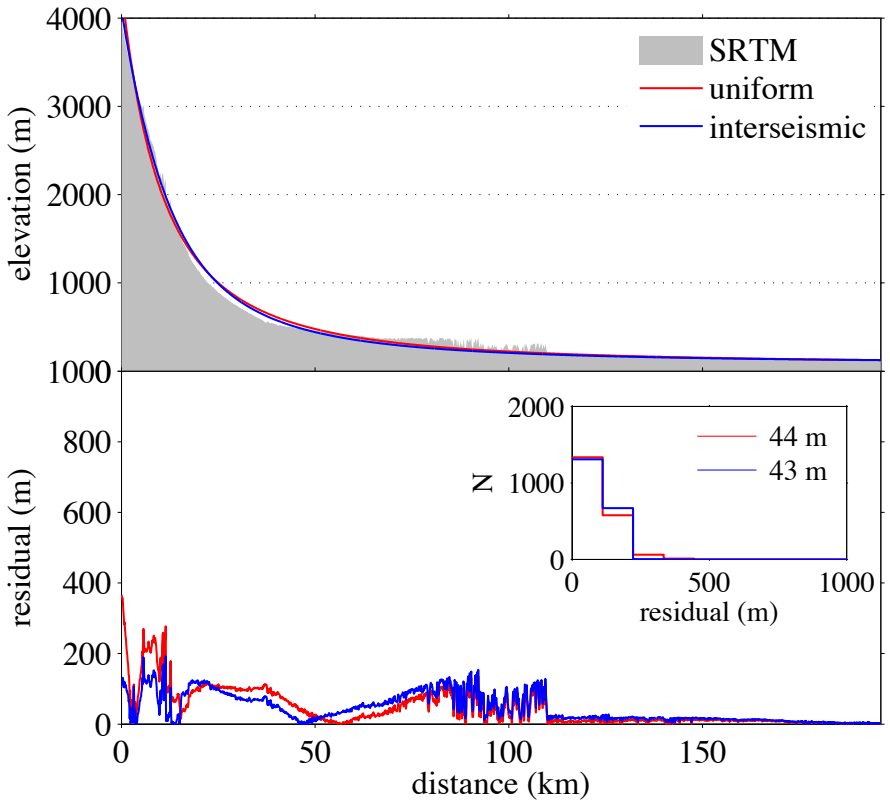

Figure DR6. Observed and modeled channel profiles for channel 5 in Figure DR1. Upper panel: Raw elevation data (SRTM) is shown in gray with uniform and excess interseismic rock uplift models in red and black respectively. Lower panel: magnitude of residual (SRTM-modeled) elevations for uniform (red) and excess interseismic (blue) rock uplift models. Residual elevation frequency distribution shown in inset. Legend gives the mean residual magnitude for uniform (red) and excess interseismic (blue) rock uplift models.

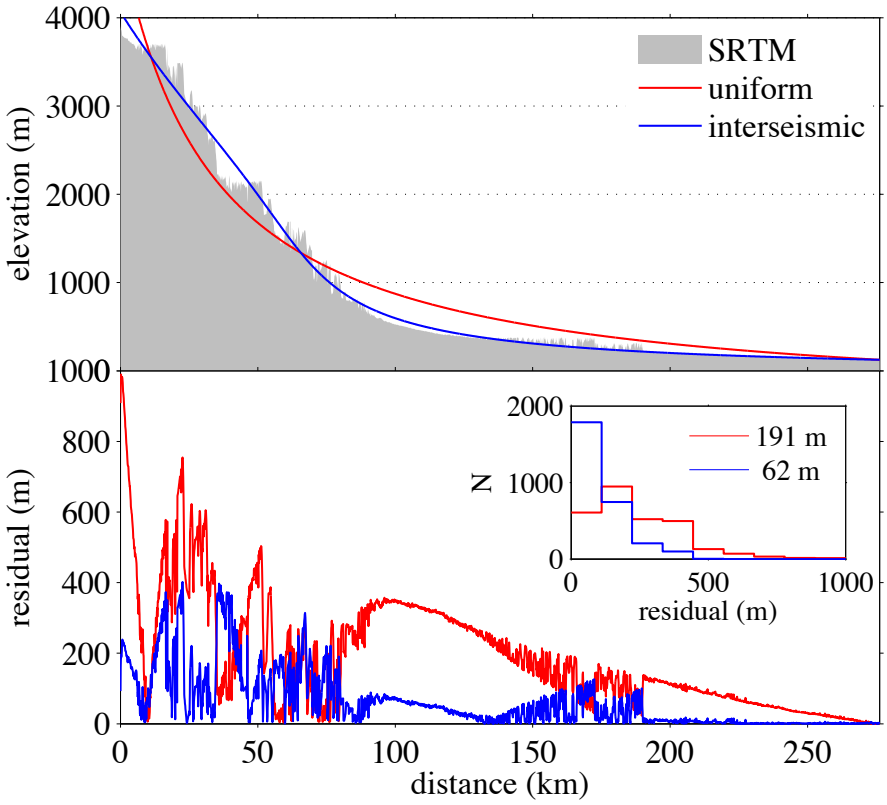

Figure DR7. Observed and modeled channel profiles for channel 6 in Figure DR1. Upper panel: Raw elevation data (SRTM) is shown in gray with uniform and excess interseismic rock uplift models in red and black respectively. Lower panel: magnitude of residual (SRTM-modeled) elevations for uniform (red) and excess interseismic (blue) rock uplift models. Residual elevation frequency distribution shown in inset. Legend gives the mean residual magnitude for uniform (red) and excess interseismic (blue) rock uplift models.

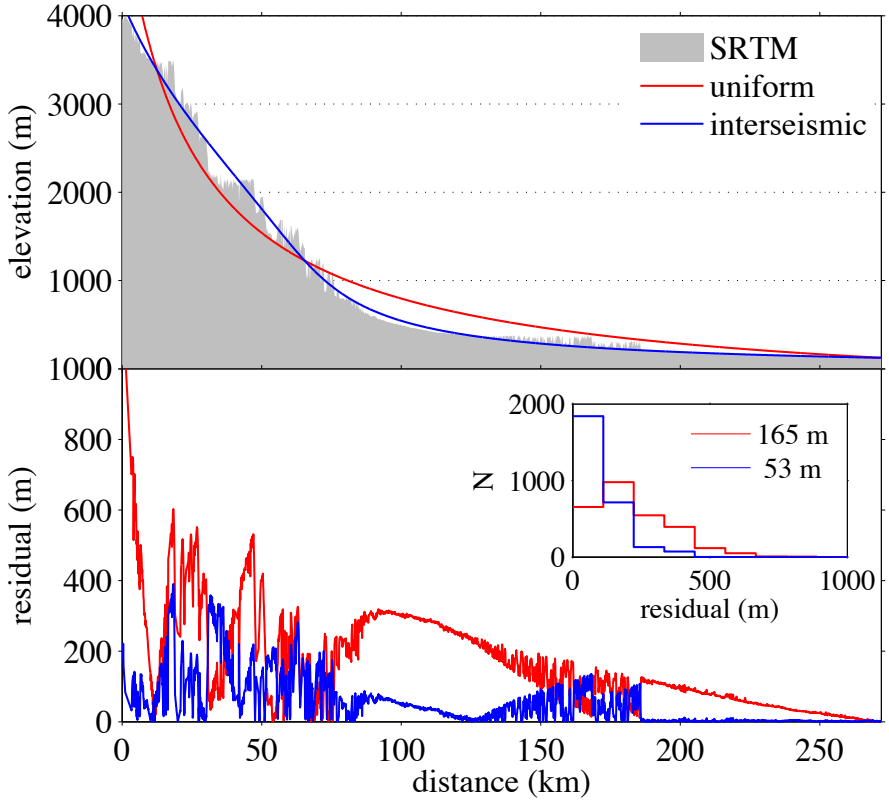

Figure DR8. Observed and modeled channel profiles for channel 7 in Figure DR1. Upper panel: Raw elevation data (SRTM) is shown in gray with uniform and excess interseismic rock uplift models in red and black respectively. Lower panel: magnitude of residual (SRTM-modeled) elevations for uniform (red) and excess interseismic (blue) rock uplift models. Residual elevation frequency distribution shown in inset. Legend gives the mean residual magnitude for uniform (red) and excess interseismic (blue) rock uplift models.

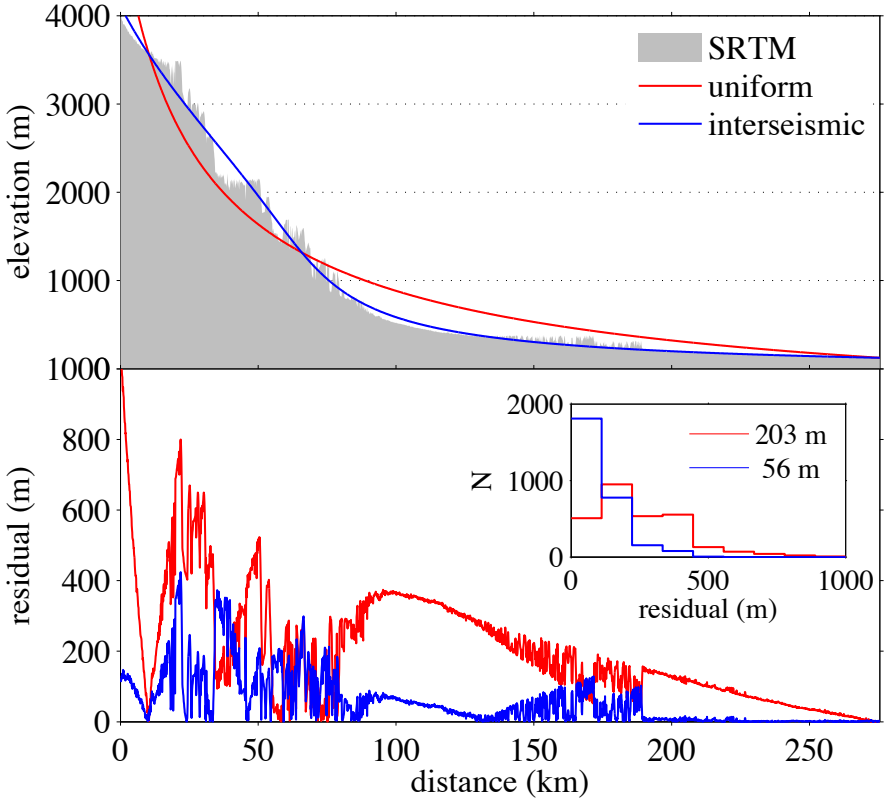

Figure DR9. Observed and modeled channel profiles for channel 8 in Figure DR1. Upper panel: Raw elevation data (SRTM) is shown in gray with uniform and excess interseismic rock uplift models in red and black respectively. Lower panel: magnitude of residual (SRTM-modeled) elevations for uniform (red) and excess interseismic (blue) rock uplift models. Residual elevation frequency distribution shown in inset. Legend gives the mean residual magnitude for uniform (red) and excess interseismic (blue) rock uplift models.

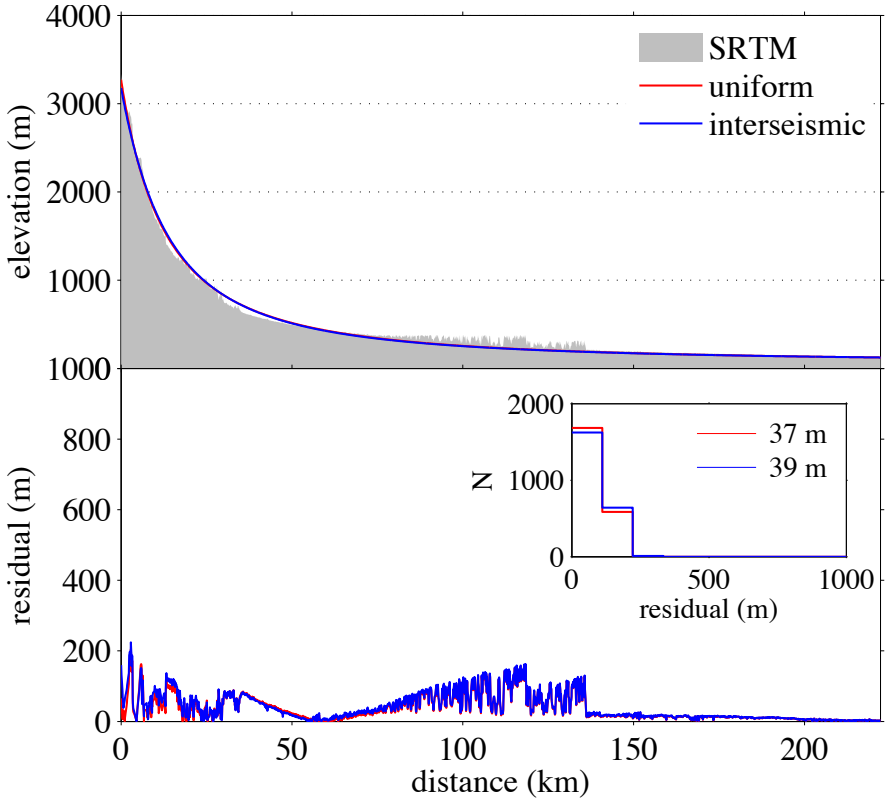

Figure DR10. Observed and modeled channel profiles for channel 9 in Figure DR1. Upper panel: Raw elevation data (SRTM) is shown in gray with uniform and excess interseismic rock uplift models in red and black respectively. Lower panel: magnitude of residual (SRTM-modeled) elevations for uniform (red) and excess interseismic (blue) rock uplift models. Residual elevation frequency distribution shown in inset. Legend gives the mean residual magnitude for uniform (red) and excess interseismic (blue) rock uplift models.

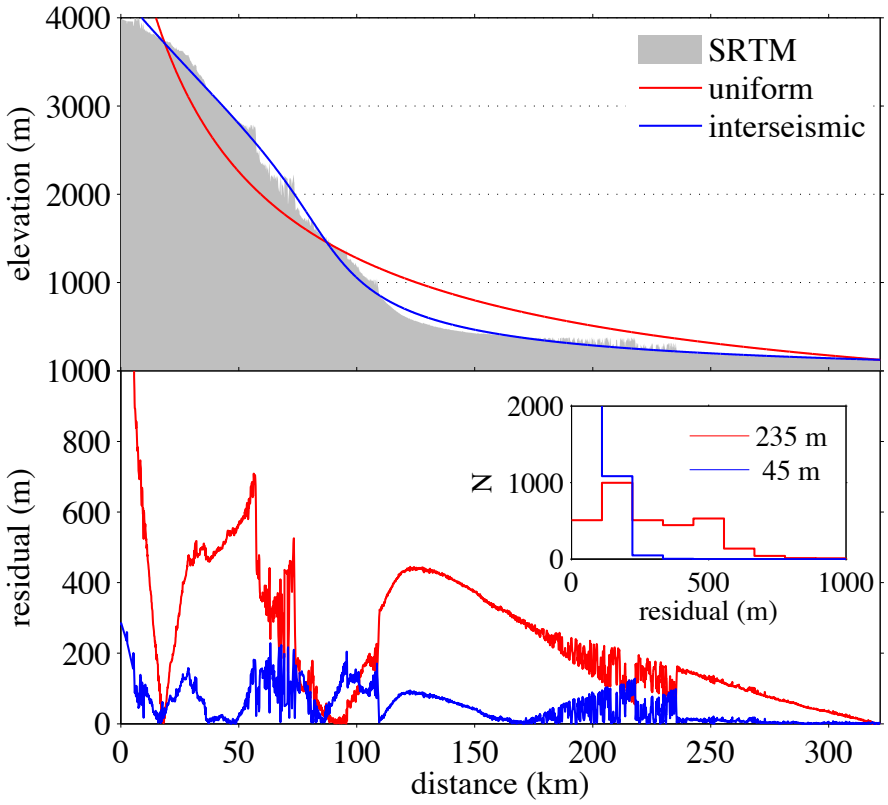

Figure DR11. Observed and modeled channel profiles for channel 10 in Figure DR1. Upper panel: Raw elevation data (SRTM) is shown in gray with uniform and excess interseismic rock uplift models in red and black respectively. Lower panel: magnitude of residual (SRTM-modeled) elevations for uniform (red) and excess interseismic (blue) rock uplift models. Residual elevation frequency distribution shown in inset. Legend gives the mean residual magnitude for uniform (red) and excess interseismic (blue) rock uplift models.

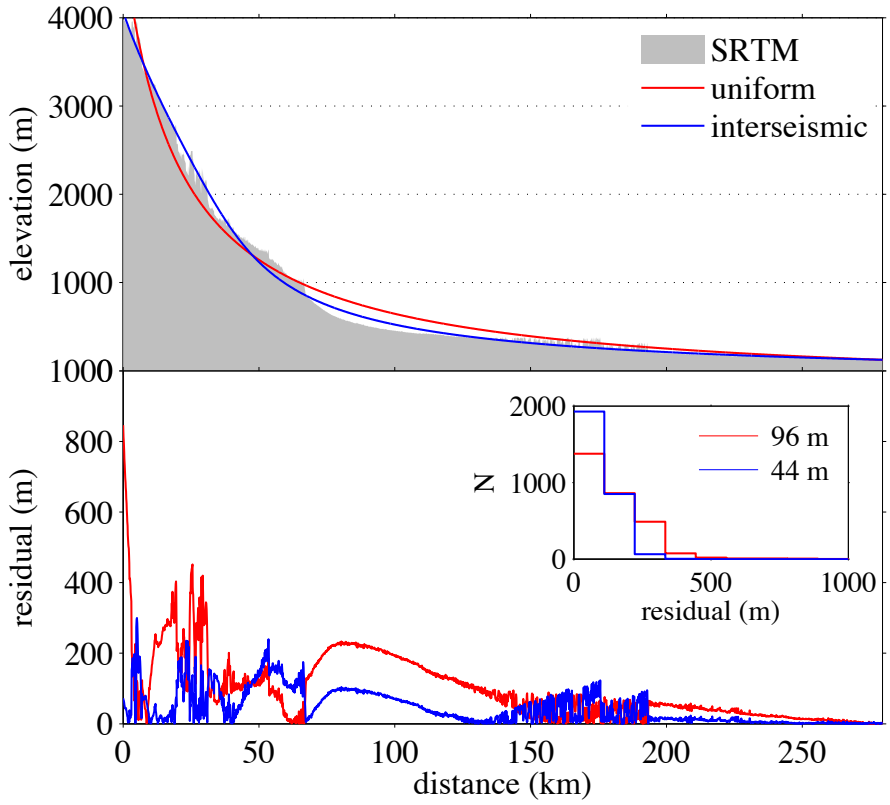

Figure DR12. Observed and modeled channel profiles for channel 11 in Figure DR1. Upper panel: Raw elevation data (SRTM) is shown in gray with uniform and excess interseismic rock uplift models in red and black respectively. Lower panel: magnitude of residual (SRTM-modeled) elevations for uniform (red) and excess interseismic (blue) rock uplift models. Residual elevation frequency distribution shown in inset. Legend gives the mean residual magnitude for uniform (red) and excess interseismic (blue) rock uplift models.

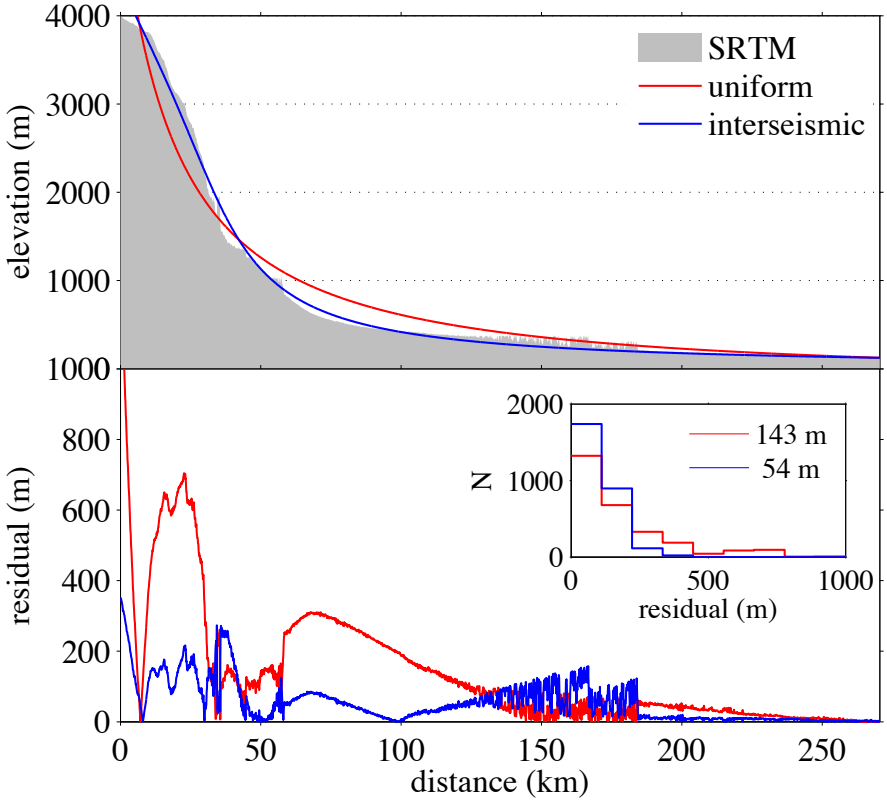

Figure DR13. Observed and modeled channel profiles for channel 12 in Figure DR1. Upper panel: Raw elevation data (SRTM) is shown in gray with uniform and excess interseismic rock uplift models in red and black respectively. Lower panel: magnitude of residual (SRTM-modeled) elevations for uniform (red) and excess interseismic (blue) rock uplift models. Residual elevation frequency distribution shown in inset. Legend gives the mean residual magnitude for uniform (red) and excess interseismic (blue) rock uplift models.

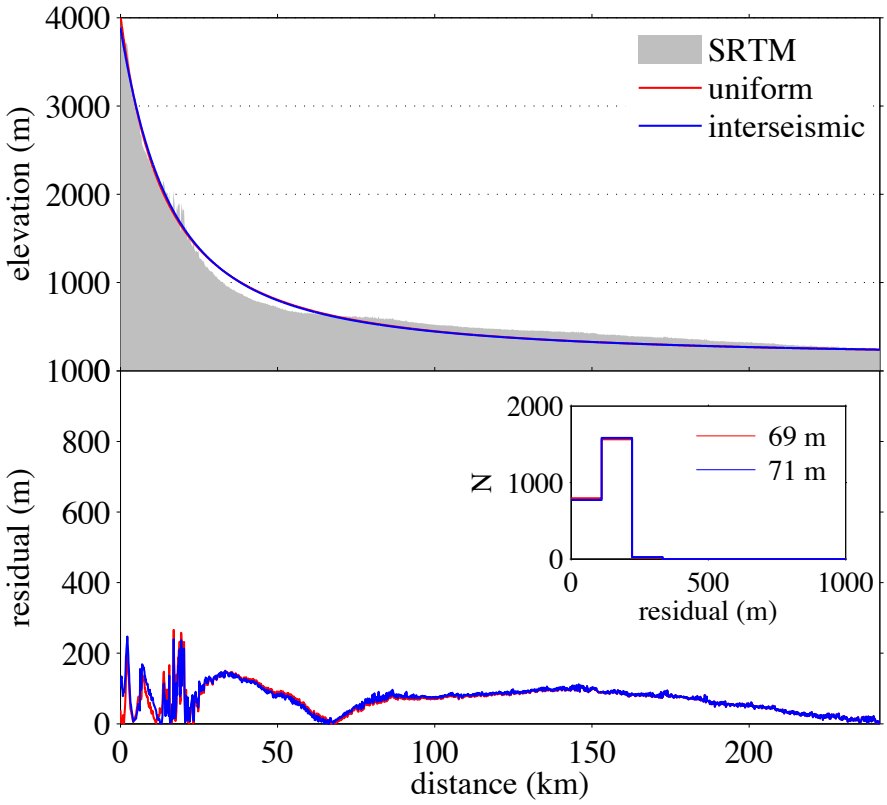

Figure DR14. Observed and modeled channel profiles for channel 13 in Figure DR1. Upper panel: Raw elevation data (SRTM) is shown in gray with uniform and excess interseismic rock uplift models in red and black respectively. Lower panel: magnitude of residual (SRTM-modeled) elevations for uniform (red) and excess interseismic (blue) rock uplift models. Residual elevation frequency distribution shown in inset. Legend gives the mean residual magnitude for uniform (red) and excess interseismic (blue) rock uplift models.

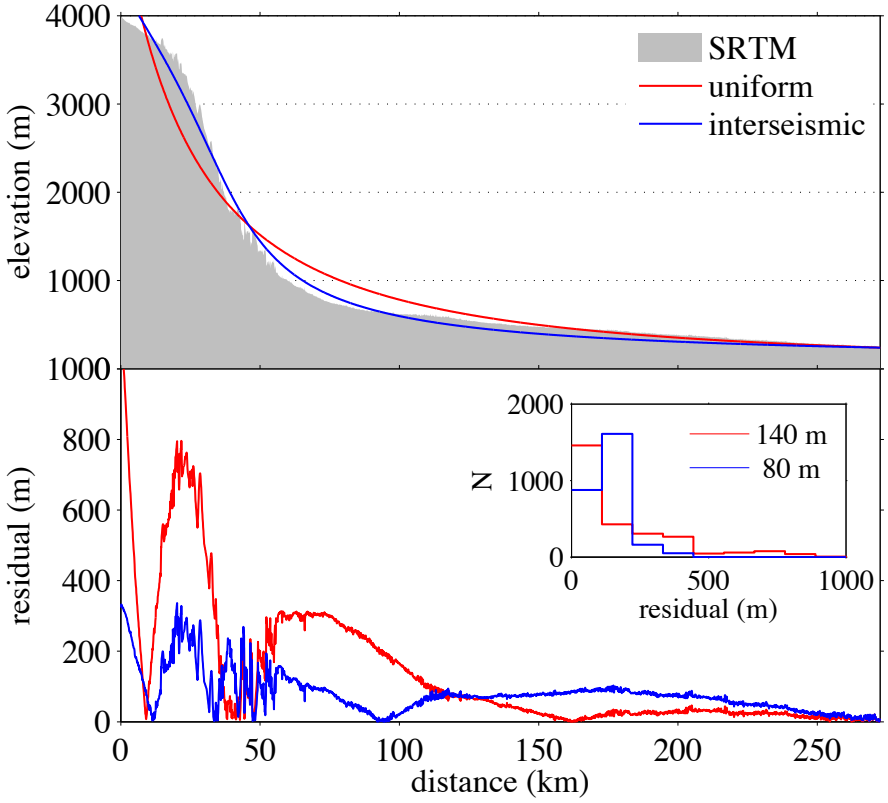

Figure DR15. Observed and modeled channel profiles for channel 14 in Figure DR1. Upper panel: Raw elevation data (SRTM) is shown in gray with uniform and excess interseismic rock uplift models in red and black respectively. Lower panel: magnitude of residual (SRTM-modeled) elevations for uniform (red) and excess interseismic (blue) rock uplift models. Residual elevation frequency distribution shown in inset. Legend gives the mean residual magnitude for uniform (red) and excess interseismic (blue) rock uplift models.

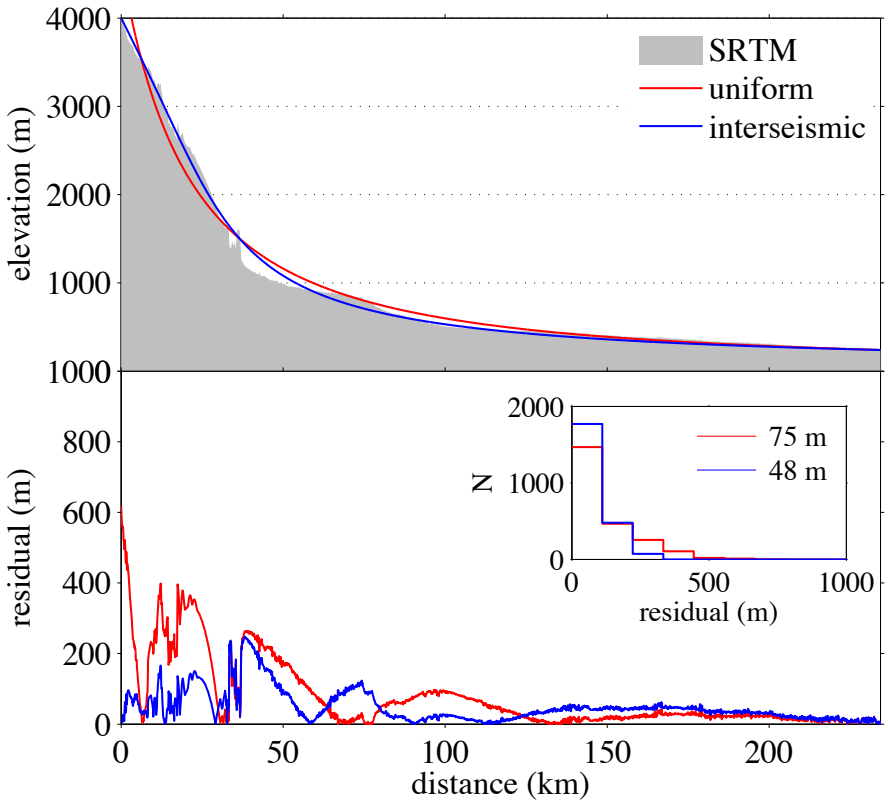

Figure DR16. Observed and modeled channel profiles for channel 15 in Figure DR1. Upper panel: Raw elevation data (SRTM) is shown in gray with uniform and excess interseismic rock uplift models in red and black respectively. Lower panel: magnitude of residual (SRTM-modeled) elevations for uniform (red) and excess interseismic (blue) rock uplift models. Residual elevation frequency distribution shown in inset. Legend gives the mean residual magnitude for uniform (red) and excess interseismic (blue) rock uplift models.

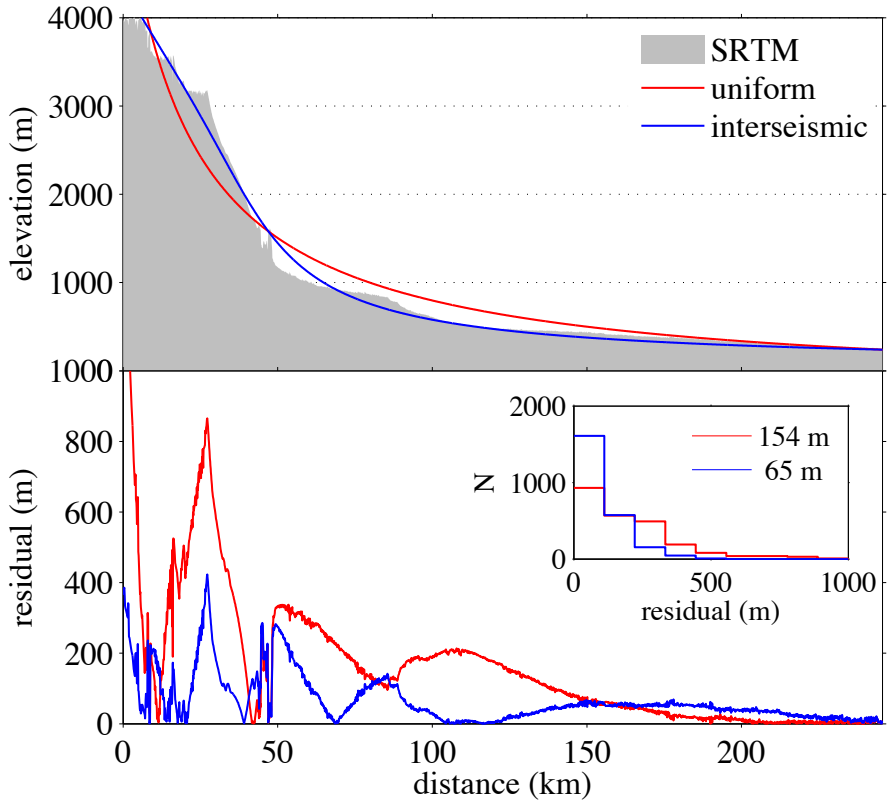

Figure DR17. Observed and modeled channel profiles for channel 16 in Figure DR1. Upper panel: Raw elevation data (SRTM) is shown in gray with uniform and excess interseismic rock uplift models in red and black respectively. Lower panel: magnitude of residual (SRTM-modeled) elevations for uniform (red) and excess interseismic (blue) rock uplift models. Residual elevation frequency distribution shown in inset. Legend gives the mean residual magnitude for uniform (red) and excess interseismic (blue) rock uplift models.

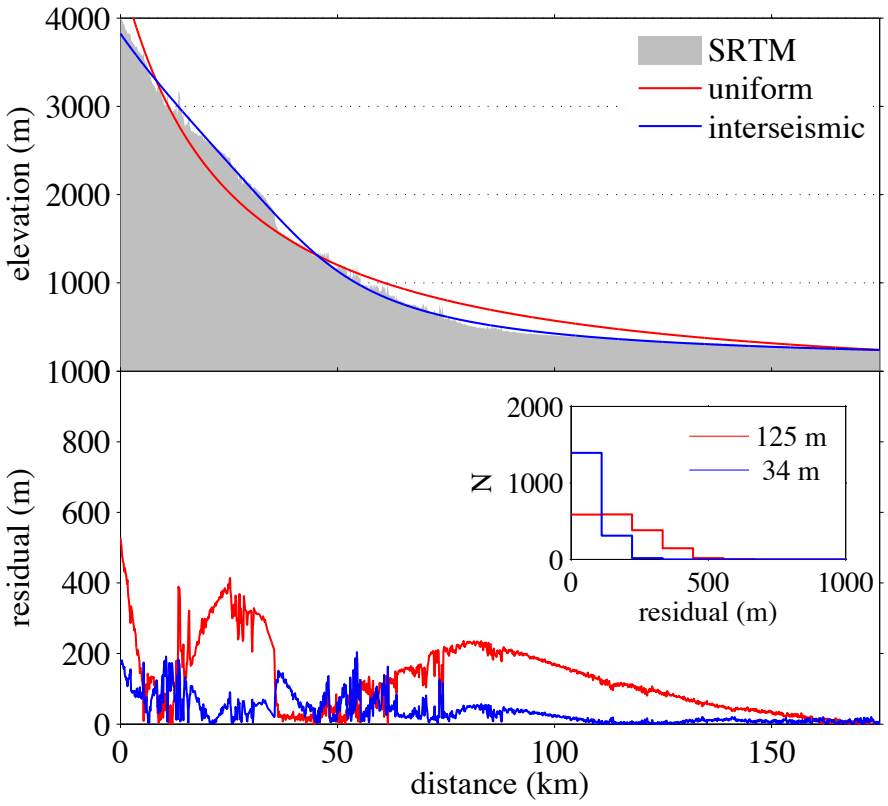

Figure DR18. Observed and modeled channel profiles for channel 17 in Figure DR1. Upper panel: Raw elevation data (SRTM) is shown in gray with uniform and excess interseismic rock uplift models in red and black respectively. Lower panel: magnitude of residual (SRTM-modeled) elevations for uniform (red) and excess interseismic (blue) rock uplift models. Residual elevation frequency distribution shown in inset. Legend gives the mean residual magnitude for uniform (red) and excess interseismic (blue) rock uplift models.

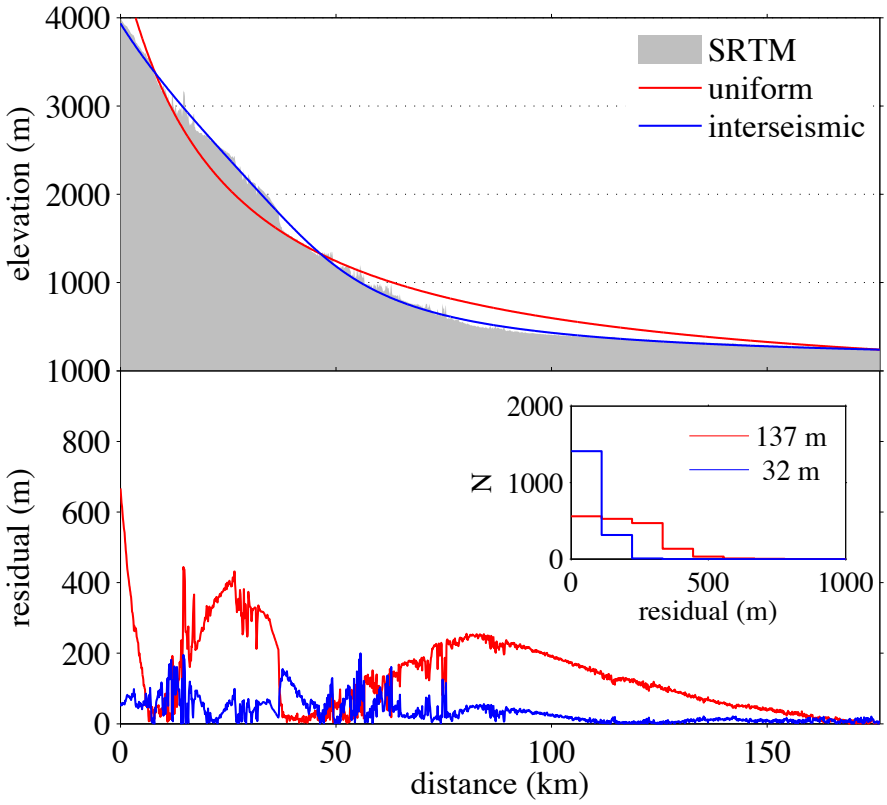

Figure DR19. Observed and modeled channel profiles for channel 18 in Figure DR1. Upper panel: Raw elevation data (SRTM) is shown in gray with uniform and excess interseismic rock uplift models in red and black respectively. Lower panel: magnitude of residual (SRTM-modeled) elevations for uniform (red) and excess interseismic (blue) rock uplift models. Residual elevation frequency distribution shown in inset. Legend gives the mean residual magnitude for uniform (red) and excess interseismic (blue) rock uplift models.

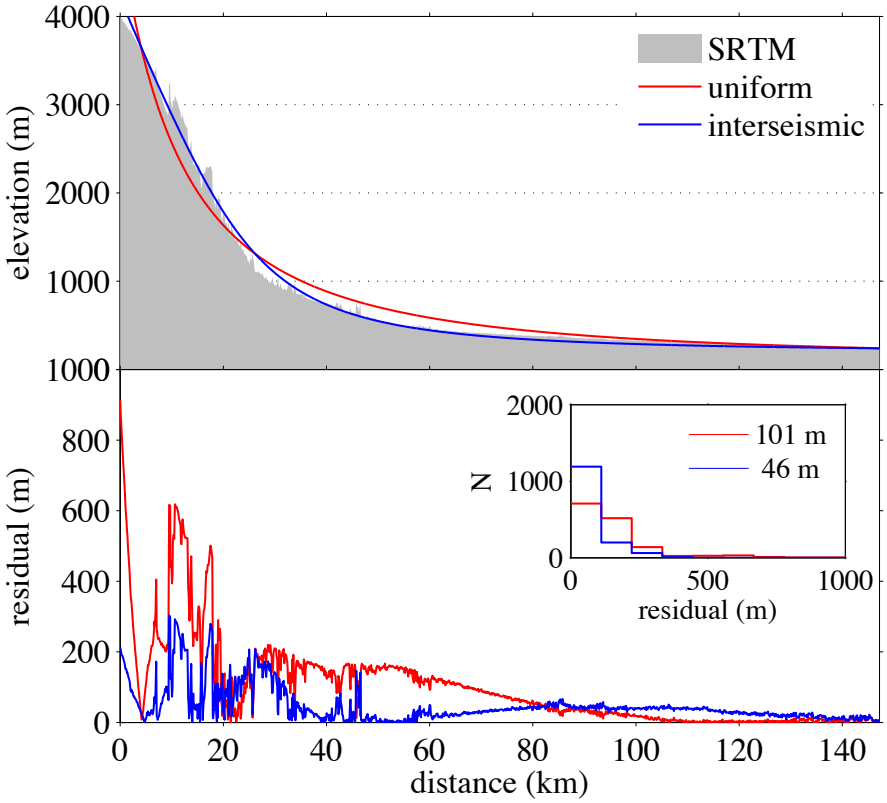

Figure DR20. Observed and modeled channel profiles for channel 19 in Figure DR1. Upper panel: Raw elevation data (SRTM) is shown in gray with uniform and excess interseismic rock uplift models in red and black respectively. Lower panel: magnitude of residual (SRTM-modeled) elevations for uniform (red) and excess interseismic (blue) rock uplift models. Residual elevation frequency distribution shown in inset. Legend gives the mean residual magnitude for uniform (red) and excess interseismic (blue) rock uplift models.

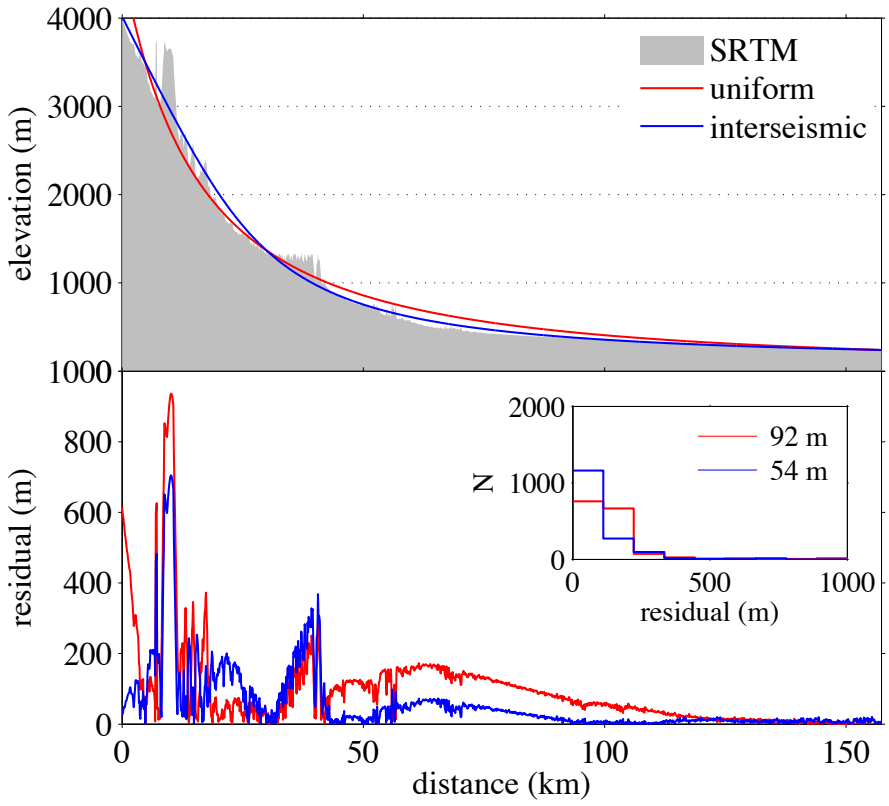

Figure DR21. Observed and modeled channel profiles for channel 20 in Figure DR1. Upper panel: Raw elevation data (SRTM) is shown in gray with uniform and excess interseismic rock uplift models in red and black respectively. Lower panel: magnitude of residual (SRTM-modeled) elevations for uniform (red) and excess interseismic (blue) rock uplift models. Residual elevation frequency distribution shown in inset. Legend gives the mean residual magnitude for uniform (red) and excess interseismic (blue) rock uplift models.

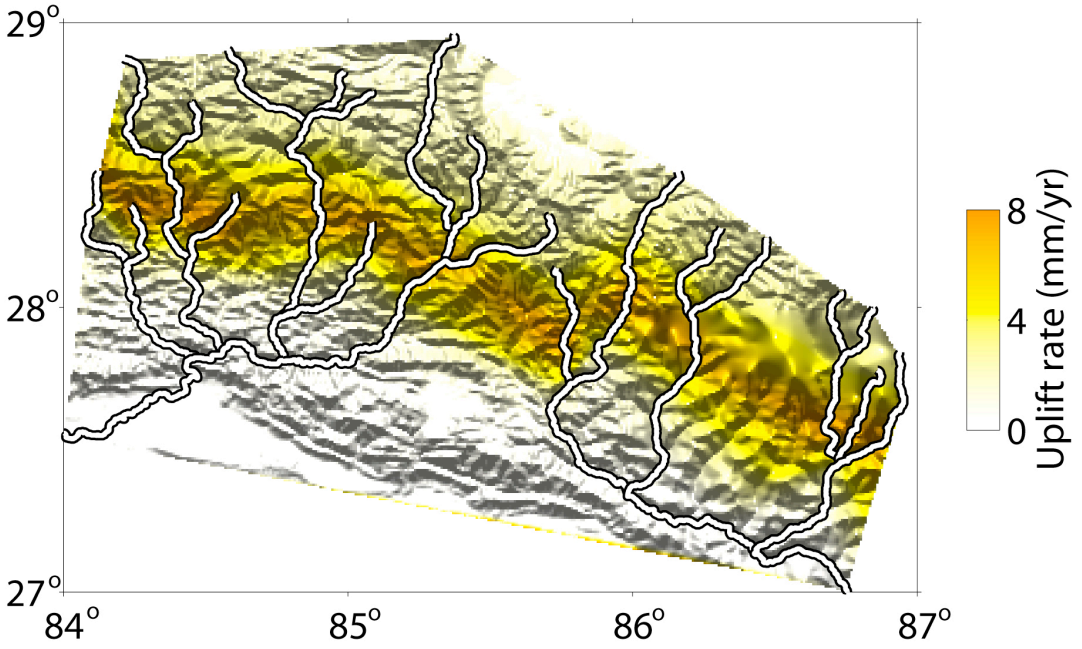

Figure DR22. Shaded relief, topographically constrained uplift rates, and channel locations. Estimated uplift rates along each channel were interpolated over the convex hull area surrounding the selected channels. The interpolated uplift field provides a means for assessing the spatial consistency of the uplift distributions constrained independently for each channel.